Brazilian Journal
of Chemical
Engineering

ISSN 0104-6632
Printed in Brazil
www.abeq.org.br/bjche

Vol. 31, No. 01, pp. 171 - 182, January - March, 2014

INVESTIGATION OF ADSORPTION OF THE DYESTUFF ASTRAZON RED VIOLET 3RN (BASIC VIOLET 16) ON MONTMORILLONITE CLAY

B. A. Fil[1,2*], M. T. Yilmaz[1], S. Bayar[1] and M. T. Elkoca[1]

[1]Atatürk University, Faculty of Engineering, Department of Environmental Engineering, 25240, Erzurum - Turkey.
Phone: + 90 442 2314812, Fax: + 90 442 2314806.
E-mail: baybarsalifil2@gmail.com
[2]Balıkesir University, Faculty of Engineering, Department of Environmental Engineering, 10145, Balıkesir - Turkey.

(Submitted: April 25, 2012 ; Accepted: March 27, 2013)

Abstract - In this study, color removal by absorption from synthetically prepared wastewater was investigated using montmorillonite clay by adsorption. As dyestuff Astrazon Red Violet 3RN (Basic Violet 16) was used. Experimental parameters selected were pH, temperature, agitation speed, initial dyestuff concentration, adsorbent dosage and ionic strength. It was established that adsorption rate increased with increasing pH, temperature, dye concentration and agitation speed, but decreased with increased ionic strength and adsorbent dosage. Adsorption equilibrium data obtained by a series of experiments carried out in a water bath were employed with common isotherm equations such as Langmuir, Freundlich, Temkin, Elovich and Dubinin–Radushkevich. It was found that the Langmuir equation appears to fit the equilibrium data better than the other models. Furthermore, the fit of the kinetic data to common kinetic models such as the pseudo-first-order, second-order, Elovich and intraparticle diffusion models was tested to elucidate the adsorption mechanism. Kinetic data conformed to the pseudo-second-order model, indicating chemisorptions. In addition, the thermodynamic parameters activation energy, Ea, enthalpy ΔH*, entropy, ΔS*, and free energy change, ΔG*, were calculated. The values of the calculated parameters indicated that physical adsorption of ARV on the clay was dominant and that the adsorption process was endothermic.

Keywords: Adsorption; Isotherm models; Kinetic models; Montmorillonite; Thermodynamic parameters.

INTRODUCTION

In waste waters of the textile industry, dyes are major water pollutants, even in very low concentration. Dye wastewater from the dye manufacturing and textile industries may show toxic or carcinogenic effects on living things when discharged into rivers and lakes, changing their biological life (Kumar *et al.*, 1998). Textile dye wastewater can contain chemicals, salts, acids, bases, chlorinated organic compounds, and occasionally heavy metals, together with the complex dye.

Contemporarily, the most common methods of textile wastewater treatment include: adsorption (Mahmoodi, 2011), biosorption (Somasekhara Reddy *et al.*, 2012), coagulation/flocculation (Man *et al.*, 2012), ozonation (van Leeuwen *et al.*, 2009), membrane filtration (Molinari *et al.*, 2004), electrocoagulation (Aoudj *et al.*, 2010) and photocatalytic removal (Gondal *et al.*, 2012).

Adsorption is a well-known equilibrium separation process. The adsorption process has been shown to be an effective and attractive method for the treatment of industrial wastewaters containing colored dyes, heavy metals and other inorganic and organic impurities. Currently, adsorption processes have been studied because of their low cost and easy access. Also, dyes can be effectively removed by an

---

*To whom correspondence should be addressed adsorption process in which dissolved dye compounds attach themselves to the surface of adsorbents. Various adsorbents such as: activated carbon (Khaled *et al.*, 2009; Bangash and Alam, 2009; Schimmel *et al.*, 2010), flay ash (Lin *et al.*, 2008), sawdust (Bello *et al.*, 2010), lignite (Pentari *et al.*, 2009), bentonite (Bulut *et al.*, 2008), sepiolite (Dogan *et al.*, 2007), montmorillonite (Fil and Özmetin, 2012), polymers (Kim and Guiochon, 2005), resin (Coşkun, 2011), zeolite (Mesko *et al.*, 2001), macroporous hydrogel (Li *et al.*, 2010), orange peel (Mafra *et al.*, 2013), chitosan (Piccin *et al.*, 2011), etc. have been widely studied for dye removal from aqueous solution.

This study reports, for the first time, the feasibility of employing montmorillonite as a low-cost alternative adsorbent for Astrazon Red Violet 3RN (basic violet 16) color removal from aqueous solution. The effects of the initial ARV concentration, pH, agitation speed, adsorbent dosage, ionic strength and reaction temperature on ARV adsorption onto montmorillonite were studied. Adsorption isotherms, kinetics, and thermodynamic parameters were also evaluated and discussed.

MATERIALS AND METHODS

Materials

Samples of montmorillonite were obtained from Süd-Chemie (Balikesir, Turkey). The chemical composition and physical properties of montmorillonite are given in Table 1 (Fil, 2007). All reagents used were of at least analytical grade.

Table 1: Chemical composition of montmorillonite (a) and physicochemical properties of montmorillonite (b).

	Component	Weight (%)
(a)	SiO_2	49.40
	Al_2O_3	19.70
	MgO	0.27
	CaO	1.50
	Fe_2O_3	0.30
	Na_2O	1.50
	H_2O	25.67
	Parameters	**Value**
(b)	Color	White
	Density (g cm^{-3})	2.3 - 3
	Transparency	Semi-transparent and opaque
	Brightness	Matt
	Surface Area (m^2 g^{-1})	95.36
	Reflective index	1 - 2

ARV (basic violet 16) dye was obtained from Dyestar (Frankfurt, Germany) and has the chemical structure shown in Figure 1 (molecular weight 368.943 g mol^{-1} and molecular formula $C_{23}H_{29}ClN_2$) (Rashidian *et al.*, 2009).

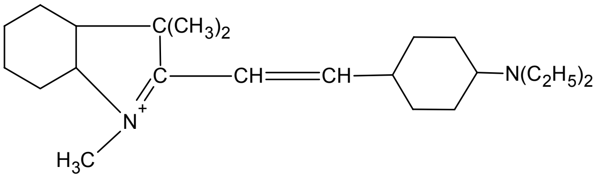

Figure 1: The structure of Astrazon Red Violet 3RN (basic violet 16).

Methods

The effects of variables including pH, agitation speed, temperature, ionic strength, adsorbent dosage, contact time and initial dye concentration on the adsorptive removal of Astrazon Red Violet 3RN were investigated in batch mode. In each experimental run, 100 mL of ARV solution of different concentrations from 25 mg L^{-1} to 750 mg L^{-1} and varying amounts montmorillonite were kept in a 250 ml erlenmeyer flask. Constant agitation speeds (Edmund Bühler) from 100 rpm to 400 rpm and temperatures from 293 K to 333 K were maintained for all the adsorption experiments. Ionic strength of aqueous solutions was adjusted with NaCl. The solution pH was adjusted by addition of dilute aqueous solutions of HCl (0.01M) or NaOH (0.01M) using a WTW multi 340i pH-meter. Samples were taken at different contact times to determine the time required to reach equilibrium. After centrifugation at 10000 rpm, the absorbance of the supernatant was measured at 530 nm (Rashidian *et al.*, 2009) (Spekol-1100 UV-Vis spectrophotometer) and then converted into concentration.

The adsorption equilibrium of ARV was calculated using the following relationship:

$$q_e = \frac{(C_0 - C_e).V}{m} \tag{1}$$

where C_0 (mg L^{-1}) and C_t (mg L^{-1}) are the initial dye concentration and after the equilibrium time, respectively. V is the volume of the solution (L) and m is the mass (g) of montmorillonite.

The adsorption capacity of ARV was calculated for kinetic studies by the following equation:

$$q_t = \frac{\left(C_0 - C_t\right).V}{m} \tag{2}$$

where C_0 (mg L^{-1}) and C_t (mg L^{-1}) are the initial dye concentration and that after time t, respectively.

RESULTS AND DISCUSSION

Adsorption Isotherm Models

In these experiments, 0.05 g of montmorillonite was added to 100 mL of different initial dye concentration solutions. After adsorption, the new dyestuff concentration C_e (mg L^{-1}) was used to calculate the equilibrium dyestuff concentration adsorption q_e (mg g^{-1}) using Eq. (1).

Generally experimental adsorption measurement results can be expressed with an equilibrium adsorption isotherm (Aroguz *et al.*, 2008).

Adsorption of ARV at equilibrium was studied as a function of concentration and is shown in Figure 2. Adsorption of dye molecules onto the adsorbent particles rapidly increases with increasing initial dye concentration, then reaches a plateau. This is the maximum adsorption capacity (q_{max}) of the adsorbent material. The maximum adsorption capacity of Astrazon Red Violet 3RN on montmorillonite was calculated as 526.149 mg g^{-1}. The equilibrium dye adsorption increases with increasing initial dyestuff concentration (Gurses *et al.*, 2006).

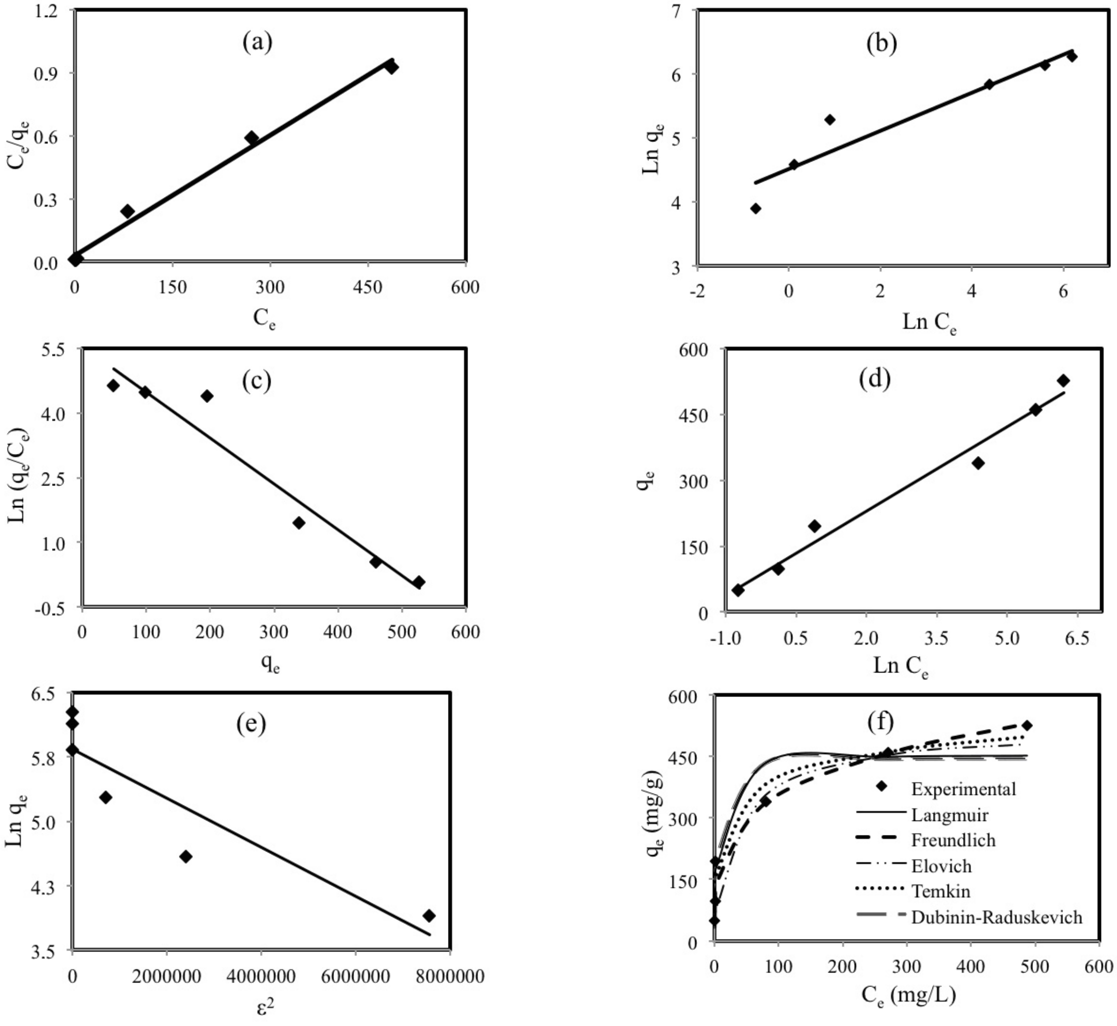

Figure 2: Comparison of isotherm models for dye adsorption on montmorillonite (a) Langmuir, (b) Freundlich, (c) Elovich, (d) Temkin, (e) Dubinin Radushkevich, (f) All isotherm models, non-linear plot).

Adsorption isotherms describe the equilibrium requirement for a molecule to adsorb on the adsorbent surface (Langmuir, 1918; Doğan, 2001). To decide which isotherm will better describe the adsorption, all of the experimental data has to be analyzed with all of the isotherm equations. The most frequently used isotherms for explaining the adsorption processes are the Freundlich, Langmuir, Temkin, Elovich and Dubinin–Radushkevich isotherms (Table 2) (Dubinin and Radushkevich, 1947; Elovich and Larionov, 1962; Freundlich, 1906; Langmuir, 1918; Temkin, 1941). The best fit model was selected based on the determination coefficient (R^2). The graphs of all isotherm models are shown in Figure 2; the correlation coefficients and the values of intercept were collected in Table 3. Furthermore, as seen from Table 3 and Figure 2, correlation coefficients were highest for the Langmuir isotherm model (R^2=0.9901). The Langmuir isotherm is based on the assumption that maximum adsorption corresponds to a saturated monolayer of dye molecules on the adsorbent surface. The energy of adsorption is constant and there is no transmigration of adsorbate in the plane of the surface of montmorillonite (Fil *et al.*, 2012; Kuleyin and Aydin, 2011; Tehrani-Bagha *et al.*, 2011).

Adsorption Kinetic Models

Numerous kinetic models explaining the mechanism by which pollutants are adsorbed have been suggested (Table 4) (Chien and Clayton, 1980; Ho and McKay, 1998; Lagergren and Svenska, 1898; Weber and Morris, 1963). The kinetics of adsorption is important because this is what controls the efficiency of the process.

Table 2: Isotherm models.

Isotherm model	Linear form	Eq.	Plots	Ref.
Langmuir	$\frac{C_e}{q_e}=\frac{1}{q_m K_L}+\frac{C_e}{q_m}$	(3)	(C_e/q_e) versus C_e	Langmuir (1918)
Freundlich	$\ln q_e=\ln K_F+\frac{1}{n}\ln C_e$	(4)	$\ln q_e$ versus $\ln C_e$	Freundlich (1906)
Temkin	$q_e=\frac{RT}{b}\ln K_T+\frac{RT}{b}\ln C_e$	(5)	q_e versus $\ln C_e$	Temkin (1941)
Elovich	$\ln\frac{q_e}{C_e}=\ln(K_E q_m)-\frac{1}{q_m}q_e$	(6)	$\ln(q_e/C_e)$ versus q_e	Elovich and Larionov (1962)
Dubinin – Radushkevich	$\ln q_e=\ln q_m-B\left(RT\ln\left(1+1/C_e\right)\right)^2$	(7)	$\ln q_e$ versus $(RT\ln(1+1/C_e))^2$	Dubinin and Radushkevich (1947)

Table 3: Isotherm constants for Astrazon Red Violet 3RN adsorption onto montmorillonite.

Langmuir isotherm		Freundlich isotherm	
K_L	0.0632	K_F	91.4305
q_m	524.5737	n	3.3731
R^2	0.990	R^2	0.905
Temkin isotherm		**Elovich isotherm**	
K_T	4.9035	q_m	93.9622
b	37.9950	K_E	1.0608
R^2	0.978	R^2	0.944
Dubinin-Radushkevich isotherm			
q_m	342.3340		
B	2.86×10^{-7}		
R^2	0.825		

Table 4: Kinetic models.

Kinetic model	Linear form	Eq.	Plots	Ref.
Pseudo-first-order	$\ln(q_e - q_t) = \ln q_e - k_1 t$	(8)	Ln $(q_e$-$q_t)$ versus t	Lagergren and Svenska (1898)
Pseudo-second-order	$\frac{t}{q_t} = \left[\frac{1}{k_2 q_e^2}\right] + \frac{1}{q_e} t$	(9)	t/q_t versus t	Ho and McKay (1998)
Elovich	$q_t = \frac{1}{\beta}\ln(\alpha\beta) + \frac{1}{\beta}\ln t$	(10)	q_t versus ln t	Chien and Clayton, (1980)
Intra-particle Diffusion	$q_t = k_{dif} t^{1/2} + C$	(11)	q_t versus $t^{1/2}$	Weber and Morris, (1963)

The correlation coefficient R^2 showed that the pseudo-second-order model, indicative of a chemisorptions mechanism, fit the experimental data slightly better than the Elovich and the pseudo-first order models. In other words, the adsorption of ARV could be approximated more favorably by the pseudo- second-order kinetic model (Ho and McKay, 1998a,b). The calculated k_2 (g mg^{-1} min^{-1}) and R^2 values are listed in Table 5 and plots for all the kinetic models are shown in Figure 3. Similar results were found for methylene blue adsorption onto montmorillonite (Fil and Özmetin, 2012), methylene blue and crystal violet adsorption onto palygorskite (Al-Futaisi *et al.*, 2007), basic yellow 28, methylene blue, and malachite green adsorption onto Iranian kaolin, (Tehrani-Bagha *et al.*, 2011) and methylene blue and methyl violet adsorption onto sepiolite (Dogan *et al.*, 2007). The results also indicated that an intra-particle diffusion mechanism played a significant role in the adsorption process, while the adsorption rate was controlled by a film-diffusion step (Ugurlu and Karaoglu, 2011; Yousef *et al.*, 2011).

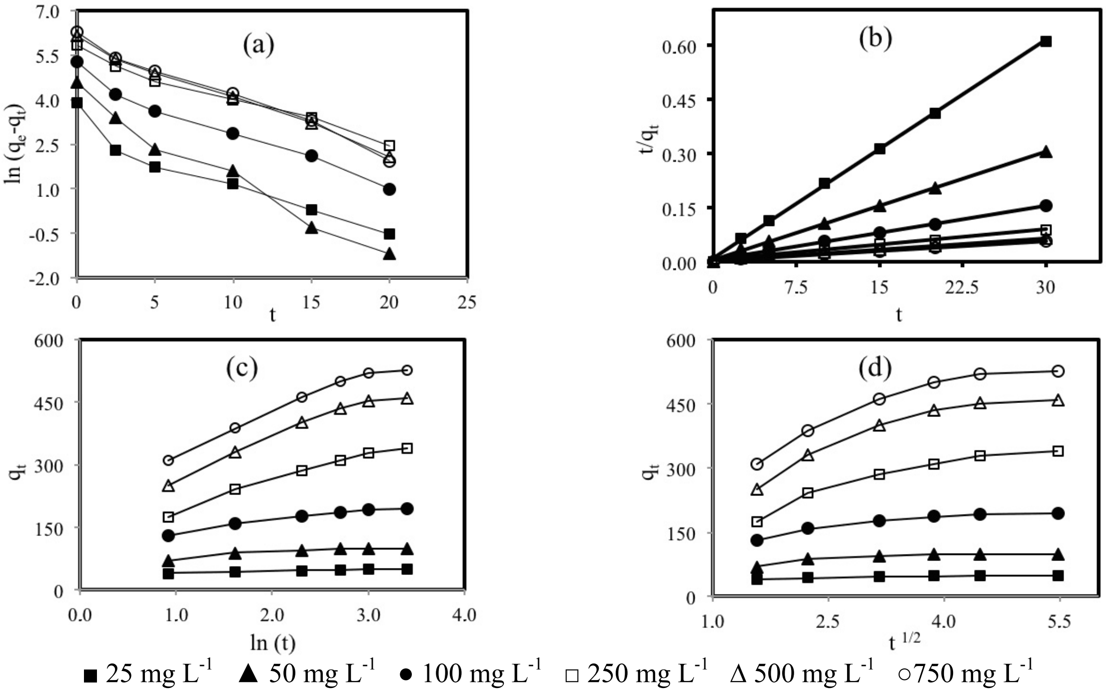

Figure 3: Comparison of kinetic models for dye adsorption on montmorillonite (a) Pseudo-first order, (b) Pseudo-second-order, (c) Elovich, (d) Intraparticle).

Table 5: Kinetic constants for Astrazon Red Violet 3RN adsorption onto montmorillonite.

Parameters						Kinetic models									
Ionic strength (mol L^{-1}NaCl)	Adsorbent dosage (g/100 ml)	Temperature (K)	Initial dye concentration (mg L^{-1})	pH	Agitation speed (rpm)	The Elovich Equation			Pseudo – first – order		Pseudo – second – order			Intra-particle	
						α mg g^{-1} min^{-1}	β g mg^{-1}	R^2	k_1 min^{-1}	R^2	$h=k_{2}xq_e^2$ mg g^{-1} min^{-1}	k_2 x 10^3 g mg^{-1} min^{-1}	R^2	k_1 mg g^{-1} $min^{-1/2}$	R^2
0	0.050	293	100	4.0	300	1907.89	0.03831	0.961	0.1953	0.972	217.108	0.005486	0.998	15.849	0.857
0	0.050	303	100	4.0	300	2781.53	0.03985	0.899	0.2038	0.960	266.411	0.006693	0.999	13.493	0.821
0	0.050	313	100	4.0	300	69550.05	0.05852	0.902	0.1670	0.902	379.939	0.009578	0.999	10.727	0.805
0	0.050	323	100	4.0	300	1584187.83	0.07478	0.925	0.2199	0.902	538.503	0.013511	1.000	8.010	0.810
0	0.050	333	100	4.0	300	454966031.91	0.09912	0.792	0.2382	0.774	1408.490	0.035278	1.000	4.095	0.646
0	0.050	293	25	4.0	300	13103.04	0.23091	0.922	0.1945	0.922	95.685	0.038846	0.999	2.4281	0.878
0	0.050	293	50	4.0	300	3493.99	0.08917	0.842	0.2804	0.975	172.058	0.017223	0.999	6.5613	0.704
0	0.050	293	100	4.0	300	1907.89	0.03831	0.961	0.1953	0.972	217.108	0.005486	0.998	15.849	0.857
0	0.050	293	250	4.0	300	424.88	0.01493	0.977	0.1567	0.982	198.570	0.001582	0.993	41.061	0.896
0	0.050	293	500	4.0	300	715.98	0.01142	0.965	0.1923	0.992	312.305	0.001356	0.995	53.293	0.872
0	0.050	293	750	4.0	300	1212.15	0.01089	0.971	0.2009	0.986	400.000	0.001335	0.996	56.132	0.885
0	0.025	293	100	4.0	300	4830.98	0.03244	0.974	0.1785	0.954	304.044	0.004481	0.998	18.845	0.889
0	0.050	293	100	4.0	300	1907.89	0.03831	0.961	0.1953	0.972	217.108	0.005486	0.998	15.849	0.857
0	0.075	293	100	4.0	300	4341.49	0.04772	0.790	0.3104	0.935	644.330	0.036273	1.000	4.0133	0.642
0	0.100	293	100	4.0	300	4645.39	0.05962	0.590	0.3854	0.795	2000.000	0.201643	1.000	0.9839	0.444
0	0.050	293	100	4.0	100	135.69	0.03181	0.980	0.1539	0.987	75.008	0.003119	0.990	19.322	0.904
0	0.050	293	100	4.0	200	291.02	0.03012	0.968	0.1910	0.993	121.521	0.003576	0.995	20.249	0.879
0	0.050	293	100	4.0	300	1907.89	0.03831	0.961	0.1953	0.971	217.108	0.005486	0.998	15.849	0.857
0	0.050	293	100	4.0	400	18473.30	0.04980	0.906	0.2671	0.966	369.549	0.009095	0.999	11.925	0.780
0	0.050	293	100	4.0	300	1907.89	0.03831	0.961	0.1953	0.972	217.108	0.005486	0.998	15.849	0.857
0	0.050	293	100	6.0	300	3732.18	0.04261	0.979	0.2018	0.963	269.251	0.006739	0.999	13.963	0.835
0	0.050	293	100	8.0	300	4432.39	0.04383	0.952	0.1728	0.913	312.402	0.007717	0.999	13.204	0.802
0	0.050	293	100	10.0	300	19653.22	0.05256	0.980	0.2349	0.953	400.320	0.009849	0.999	11.182	0.749
0.000	0.050	293	100	4.0	300	1907.67	0.03831	0.961	0.1953	0.971	217.108	0.005486	0.998	15.849	0.857
0.001	0.050	293	100	4.0	300	1319.23	0.03748	0.980	0.1514	0.937	178.508	0.004707	0.997	16.378	0.901
0.010	0.050	293	100	4.0	300	897.59	0.03652	0.986	0.1483	0.948	155.982	0.004352	0.997	16.887	0.916
0.100	0.050	293	100	4.0	300	612.19	0.03491	0.986	0.1474	0.958	136.333	0.004026	0.996	17.666	0.916

Effect of Initial Dye Concentration

The effect of initial Astrazon Red Violet 3RN (basic violet16) dyestuff concentrations on the adsorption rate was examined in the 25, 50, 100, 250, 500 and 750 mg L^{-1}concentration range at 293 K, 300 rpm agitation speed, pH: 4.0 and 0 mol L^{-1} NaCl concentration (Figure 4). These experimental results showed that the rate of adsorption on montmorillonite surface was linearly proportional to dyestuff concentration and that the adsorption capacity increased with increasing concentration.

The initial dye concentration is an important driving force. The amount of dye adsorbed increased from 49.042 mg g^{-1} to 526.149 mg g^{-1} for 0.05 g/100 mL adsorbent when the initial dye concentration was increased from 25 mg L^{-1} to 750 mg L^{-1}, respectively. It was clear that the removal of dye was dependent on the concentration of dye. Although the increase of dye concentration increased the amount of dye adsorbed, the percent color removal decreased. These results were comparable to other similar studies (Vimonses *et al.*, 2009).

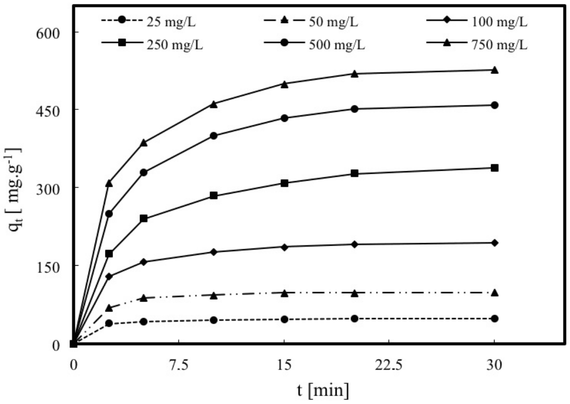

Figure 4: Effect of initial dye concentration on dye adsorption on montmorillonite (Conditions: agitation speed 300 rpm, adsorbent dosage 0.5 g L^{-1}, temperature 293 K, ionic strength 0 mol L^{-1} NaCl, solution pH: 4.0).

Effect of Initial Solution pH

The ARV dyestuff adsorption rate was examined during 30 minutes on montmorillonite samples at 293 K, 300 rpm agitation speed with solutions of initial pH 4-10 (Figure 5). These experimental results proved that the adsorption rate is linearly proportional to the starting pH value. When pH was increased from 4.0 to 10.0, the adsorption capacity increased from 194.122 mg g^{-1} to 198.569 mg g^{-1}. The solution pH value influences the adsorbent surface charge. Ion adsorption is affected by the initial solution pH value and the change in pH influence the adsorption process. Removal of ARV dyestuff on the montmorillonite surface increased with initial solution pH value. Similar results are available in the literature (Vučurović *et al.*, 2011).

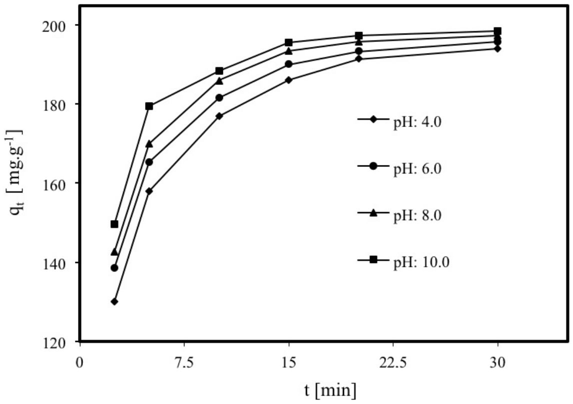

Figure 5: Effect of solution pH on dye adsorption on montmorillonite (Conditions: initial dye concentration 100 mg L^{-1}, adsorbent dosage 0.5 g L^{-1}, temperature 293 K, agitation speed 300 rpm, ionic strength 0 mol L^{-1} NaCl).

Effect of Agitation Speed

The effect of agitation speed on the Astrazon Red Violet 3RN (ARV) dyestuff adsorption rate was examined at 293 K, pH: 4.0, 0.5 g L^{-1} of adsorbent, 100 mg L^{-1} initial dyestuff concentration and agitation speeds of 100, 200, 300, and 400 rpm. Agitation speed is a very important parameter for adsorption phenomena because its effect on the outer boundary layer. For adsorption in the batch reactor, agitation quality is a very important parameter for all mass transfer processes. Figure 6 shows that the adsorption rate increased with the increase in agitation speed. When the agitation speed increased from 100 rpm to 400 rpm, the maximum adsorption capacity increased from 147.330 mg g^{-1} to 198.097 mg g^{-1}. Similar results are available in the literature (Crini *et al.*, 2007; Dogan *et al.*, 2009).

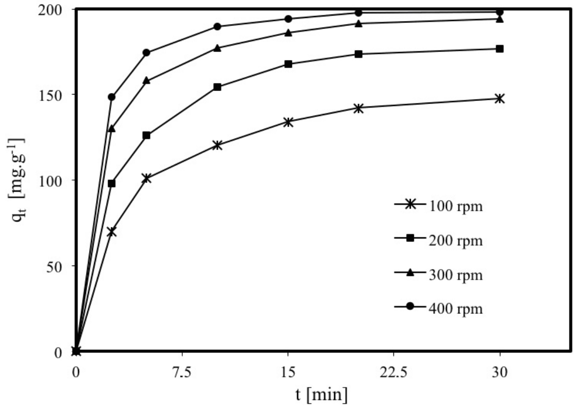

Figure 6: Effect of agitation speed on dye adsorption on montmorillonite (Conditions: initial dye concentration 100 mg L^{-1}, adsorbent dosage 0.5 g L^{-1}, temperature 293 K, ionic strength: 0 mol L^{-1} NaCl, solution pH: 4.0).

Effect of Adsorbent Dosage

The effect of adsorbent dose on the amount of dye adsorbed is shown in Figure 7. The adsorption rate of ARV onto montmorillonite in aqueous solutions was studied for montmorillonite amounts of 0.25, 0.50, 0.75 and 1.00 g L^{-1} at 293 K, 300 rpm agitation speed, 100 mg L^{-1} dyestuff concentration, 0 mol L^{-1} NaCl concentration and pH 4.0.

Figure 7 shows that the adsorption capacity decreased with increasing montmorillonite solid-liquid suspension ratio. With increasing adsorbent dosage the number of available sorption sites increases and the percentage of ARV increased too. When the adsorbent dosage increased from 0.25 g L^{-1} to 1.00 g L^{-1} removal of color increased from 63.499% to 99.402%, but the adsorption capacity decreased from 253.998 mg g^{-1} to 99.402 mg g^{-1}. This decrease in adsorption capacity could be explained by

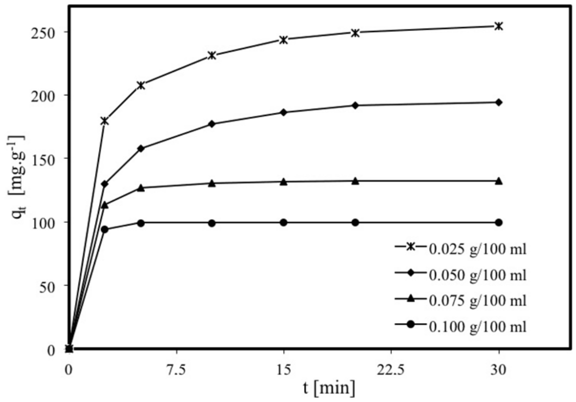

Figure 7: Effect of adsorbent dosage on dye adsorption on montmorillonite (Conditions: initial dye concentration 100 mg L^{-1}, agitation speed 300 rpm, temperature 293 K, ionic strength 0 mol L^{-1} NaCl, solution pH: 4.0).

unsaturated contaminant sorption sites during the sorption process (Varlikli *et al.*, 2009; Vimonses *et al.*, 2009).

Effect of Ionic Strength

The effect of electrolyte concentrations on the adsorption capacity of ARV on montmorillonite in aqueous solutions was examined with 0 M, 1x10^{-1} M, 1x10^{-2} M, and 1x10^{-3} M NaCl solutions at pH: 4.0, 293 K, 300 rpm agitation speed, 0.5 g L^{-1} adsorbent dosage and 100 mg L^{-1} initial dye concentration. Figure 8 shows that adsorption rate decreased with the increase in electrolyte concentration.

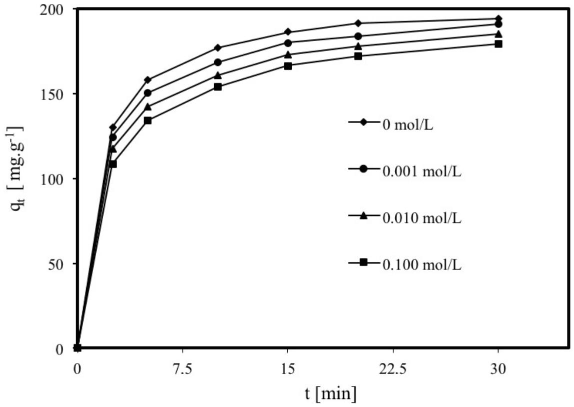

Figure 8: Effect of ionic strength on dye adsorption on montmorillonite (Conditions: initial dye concentration 100 mg L^{-1}, adsorbent dosage 0.5 g L^{-1}, temperature 293 K, agitation speed 300 rpm, solution pH: 4.0).

It is important to investigate this ion effect on adsorption because industrial wastewaters always contain contaminants like inorganic salts. Therefore, the effect of salt concentration was studied on adsorption of the dye. ARV adsorption onto the montmorillonite surface was affected negatively by NaCl in aqueous solutions. When the NaCl concentration was increased from 0 mol L^{-1} to 0.1 mol L^{-1}, the adsorption capacity decreased from 194.12 mg g^{-1} to 179.05 mg g^{-1}. Increase of the ionic strength reduces the electrostatic attraction between the adsorbate molecule and the adsorbent surface and the adsorption capacity decreases. With increasing solution ionic strength, the suspension final pH also decreased. Therefore, positive ions increase at the montmorillonite surface, screening electrostatic interactions between charges and decreasing adsorption (Dogan *et al.*, 2009; Weng *et al.*, 2009).

Effect of Solution Temperature

The effect of temperature on Astrazon Red Violet 3RN (basic violet 16) adsorption onto montmorillonite from aqueous solution was studied at 293, 303, 313, 323 and 333 K at pH 4.0, 300 rpm agitation speed, 0 M NaCl concentration, 0.5 g L^{-1} adsorbent dosage and 100 mg L^{-1} initial dye concentration. Increasing the temperature accelerates adsorbate diffusion in the outer boundary layer and adsorbent can move into the inside pores because of the solution viscosity decrease. In addition, a temperature increase or decrease will change the adsorbent capacity for a particular adsorbate.

Figure 9 shows the effect of temperature on the removal of ARV by montmorillonite. Adsorption of ARV onto montmorillonite increased from 194.12 mg g^{-1} to 199.06 mg g^{-1} with increasing temperature from 293 K to 333 K. The adsorption process was an endothermic reaction (Dogan *et al.*, 2004). The increase in dye adsorption with temperature suggests that the dye penetrates inside montmorillonite with interaction between montmorillonite hydroxyl groups and cationic groups of the dye molecule at higher temperature (Hameed and Ahmad, 2009; Karaca *et al.*, 2008).

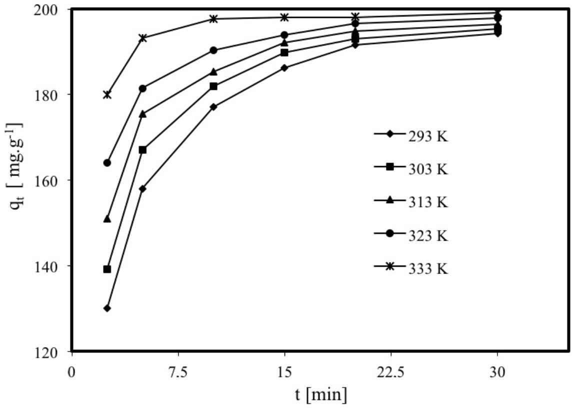

Figure 9: Effect of temperature on dye adsorption on montmorillonite (Conditions: initial dye concentration 100 mg L^{-1}, adsorbent dosage 0.5 g L^{-1}, agitation speed 300 rpm, ionic strength 0 mol L^{-1} NaCl, solution pH: 4.0).

Activation Energy and Thermodynamic Parameters

Activation Energy

The temperature dependence of the adsorption rate constant can be given as follows (Al-Ghouti *et al.*, 2005; Laidler and Meiser, 1999):

$$\ln k_2 = \ln k_0 - \frac{E_a}{R_g} \cdot \frac{1}{T} \tag{12}$$

where E_a activation energy (kJ mol^{-1}), k_0, Arrhenius constant, R_g, universal gas constant (8.314 J mol^{-1} K^{-1}).

Figure 10 shows a plot of $\ln k_2$ against to 1/T, giving a straight line. In aqueous solution, the activation energy was found to be 35.474 kJ mol^{-1} for ARV adsorption onto montmorillonite. The activation energy basically gives an idea whether adsorption is physical or chemical. A low activation energy (0–88 kJ mol^{-1}) suggests physical and a high activation energy (88–400 kJ mol^{-1}) chemical adsorption (Fil and Özmetin, 2012; Nollet *et al.*, 2003).

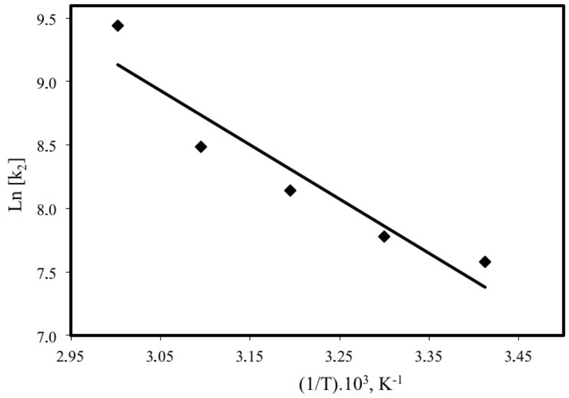

Figure 10: Arrhenius plots for adsorption of dye on montmorillonite.

Thermodynamic Parameters

Thermodynamic activation parameters for Gibbs free energy (ΔG^*), enthalpy (ΔH^*) and entropy (ΔS^*) changes were calculated using the Eyring equation (Laidler and Meiser, 1999):

$$\ln\left(\frac{k_2}{T}\right)=\left[\ln\left(\frac{k_b}{h}\right)+\frac{\Delta S^*}{R_g}\right]-\frac{\Delta H^*}{R_g}\cdot\frac{1}{T} \tag{13}$$

where, respectively, k_b and h are the Boltzmann (R_g/N, $1.38.10^{-23}$ joule mol^{-1} K^{-1}) and Planck ($6.62.10^{-34}$ joule s) constants. A plot of $\ln(k_2/T)$ against to 1/T gives a straight line with slope $-(\Delta H^*/R_g)$ and extrapolated intercept $[\ln(k_b/h)+(\Delta S^*/R_g)]$ (Figure 11). The relationship between the activation Gibbs free energy, enthalpy and entropy obey the equation:

$$\Delta G^* = \Delta H^* - T\cdot\Delta S^* \tag{14}$$

From Eq. (13), the enthalpy (ΔH^*) and entropy (ΔS^*) values were found to be, respectively, 24.003 kJ mol^{-1} and -0.0530 kJ mol^{-1} K^{-1} and the Gibbs free energy (ΔG^*) for ARV from Eq. (14) at 293 K is thus 39.541 kJ mol^{-1}. Thermodynamic coefficients are given in Table 6.

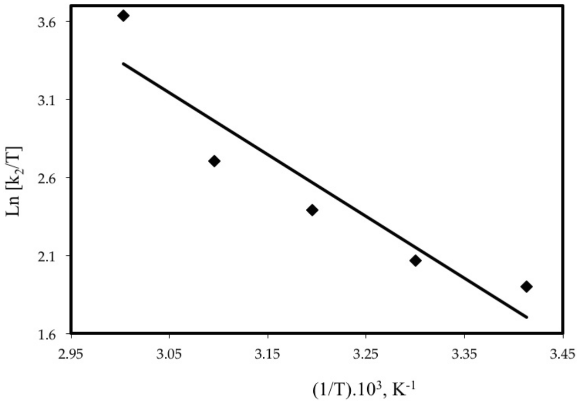

Figure 11: Plots of $\ln(k_2/T)$ versus 1/T for adsorption of dye on montmorillonite.

Table 6: Thermodynamic parameters of Astrazon Red Violet 3RN adsorption onto montmorillonite.

	T (K)				
	293	303	313	323	333
ΔG^* (kJ mol^{-1})	39.541	40.072	40.602	41.132	41.662
ΔH^* (kJ mol^{-1})	24.003				
ΔS^* (kJ mol^{-1} K^{-1})	-0.05303				

Semi-Empirical Kinetic Model

The adsorption capacity data obtained from the mass balance equation obeyed the pseudo-second-order equation, and selected parameters affected the adsorption capacity and rate. Hence, based on Eq. (9), a semi-empirical kinetic model including the effects of initial dye concentration, solution pH, agitation speed, adsorbent dosage, ionic strength, temperature, and contact time was developed by means of the Statistica 6.0 programme using 162 experimentally obtained results and is given as follows:

$$\begin{aligned}\frac{t}{q_t} &= 4.317\times\left[H^+\right]^{0.0055}\times(AS)^{-0.2412}\\ &\times(AD)^{0.8420}\times[I]^{0.0019}\times[C_0]^{-0.9561}\\ &\times\exp\left(\frac{4.267}{T}\right)\times t^{0.9252}\end{aligned} \tag{15}$$

where $[H^+]$ is hydrogen ions concentration (mol L^{-1}), (AS) is agitation speed (rpm), (AD) is the adsorbent dosage (g L^{-1}), [I] is NaCl concentration (mol L^{-1}), C_0 is the initial Astrazon Red Violet 3RN concentration (mg L^{-1}), T is the reaction temperature (K), and t is the contact time (min). The correlation between experimentally obtained (t/q_t) and predicted (t/q_t) values is given in Figure 12.

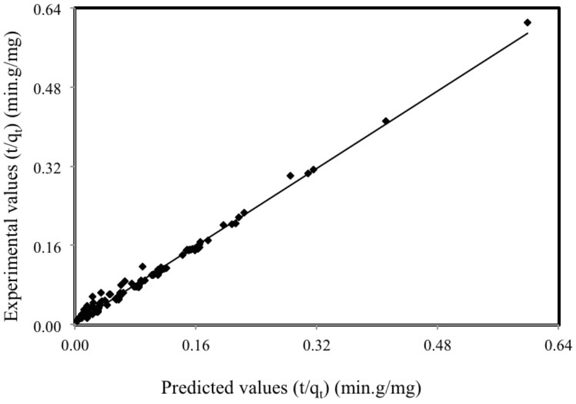

Figure 12: Correlation between experimental and statistically predicted t/q_t values.

CONCLUSIONS

From the experimental results for Astrazon Red Violet 3RN (basic violet 16) adsorption onto the montmorillonite surface it could be concluded from this study that:

- Maximum adsorption capacity was 526.149 mg g^{-1} from adsorption equilibrium experiments.
- Different adsorption isotherm models were applied and the fit of the experimental data was most suitable for the Langmuir isotherm.
- 30 minutes was enough to reach adsorption equilibrium.
- Adsorption kinetic models were applied and the pseudo-second-order kinetics model was the most suitable.
- Adsorption capacity increased with increasing pH, initial dye concentration, agitation speed and temperature and decreased with adsorbent dosage and electrolyte concentration.
- The activation energy for adsorption of ARV onto the montmorillonite surface in aqueous solution was determined to be 35.474 kJ mol^{-1}.
- The enthalpy (ΔH^*) value was 32.880 kJ mol^{-1}.
- The entropy (ΔS^*) value was -0.07116 kJ mol^{-1} K^{-1}.
- The Gibbs free energy (ΔG^*) value at 293 K was 53.731 kJ mol^{-1}.

REFERENCES

Al-Futaisi, A., Jamrah, A. and Al-Hanai, R., Aspects of cationic dye molecule adsorption to palygorskite. Desalination, 214, 327 (2007).

Al-Ghouti, M., Khraisheh, M. A. M., Ahmad, M. N. M. and Allen, S., Thermodynamic behaviour and the effect of temperature on the removal of dyes from aqueous solution using modified diatomite: A kinetic study. J. Colloid Interface Sci., 287, 6 (2005).

Aoudj, S., Khelifa, A., Drouiche, N., Hecini, M. and Hamitouche, H., Electrocoagulation process applied to wastewater containing dyes from textile industry. Chem. Eng. Process. Process Intensif., 49, 1176 (2010).

Aroguz, A. Z., Gulen, J. and Evers, R. H., Adsorption of methylene blue from aqueous solution on pyrolyzed petrified sediment. Bioresour. Technol., 99, 1503 (2008).

Bangash, F. K., Alam, S., Adsorption of acid blue 1 on activated carbon produced from the wood of *Ailanthus altissima*. Braz. J. Chem. Eng., 26, 275 (2009).

Bello, O. S., Adelaide, O. M., Hammed, M. A. and Popoola, O. A. M., Kinetic and equilibrium studies of methylene blue removal from aqueous solution by adsorption on treated sawdust. Macedonian J. Chem. Chem. Eng., 29, 77 (2010).

Bulut, E., Özacar, M. and Şengil, İ. A., Adsorption of malachite green onto bentonite: Equilibrium and kinetic studies and process design. Micropor. Mesopor. Mat., 115, 234 (2008).

Chien, S. H. and Clayton, W. R., Aplication of Elovich equation to the kinetics of phosphate release and sorption in soil. Soil Sci. Soc. Am. J., 44, 265 (1980).

Coşkun, R., Removal of cationic dye from aqueous solution by adsorption onto crosslinked poly(4-vinylpyridine/crotonic acid) and its N-oxide derivative. Polym. Bull., 67, 125 (2011).

Crini, G., Peindy, H. N., Gimbert, F. and Robert, C., Removal of CI Basic Green 4 (Malachite Green) from aqueous solutions by adsorption using cyclodextrin-based adsorbent: Kinetic and equilibrium studies. Sep. Purif. Technol., 53, 97 (2007).

Dogan, M., Alkan, M., Turkyilmaz, A. and Ozdemir, Y., Kinetics and mechanism of removal of methylene blue by adsorption onto perlite. J. Hazard. Mater., 109, 141 (2004).

Dogan, M., Karaoglu, M. H. and Alkan, M., Adsorption kinetics of maxilon yellow 4GL and maxilon red GRL dyes on kaolinite. J. Hazard. Mater., 165, 1142 (2009).

Dogan, M., Özdemir, Y. and Alkan, M., Adsorption kinetics and mechanism of cationic methyl violet and methylene blue dyes onto sepiolite. Dyes Pigm., 75, 701 (2007).

Doğan, M., The investigation of surface charge and adsorption properties of perlite in water media, Ph.D. Thesis, Balıkesir University, Balıkesir, pp. 186 (2001).

Dubinin, M. M. and Radushkevich, L. V., Equation of the characteristic curve of activated charcoal. Proc. Acad. Sci. USSR Phys. Chem. Sect., 55, 331 (1947).

Elovich, S. Y. and Larionov, O. G., Theory of adsorption from solutions of non electrolytes on solid (I) equation adsorption from solutions and the analysis of its simplest form, (II) verification of the equation of adsorption isotherm from solutions. Izv. Akad. Nauk. SSSR, Otd. Khim., 2, 209 (1962).

Fil, B. A., The Investigation of the use of montmorillonite in the removal of methylene blue, a textile dye. Master Thesis, Balikesir University, Balikesir, pp. 82 (2007).

Fil, B. A. and Özmetin, C., Adsorption of cationic dye from aqueous solution by clay as an adsorbent: Thermodynamic and kinetic studies. Journal J. Chem. Soc. Pak., 34, 896 (2012).

Fil, B. A., Özmetin, C. and Korkmaz, M., Cationic dye (methylene blue) removal from aqueous solution by Montmorillonite. Bull. Korean Chem. Soc., 33, 3184 (2012).

Freundlich, H. M. F., Over the adsorption in solution. J. Phys. Chem., 57, 385 (1906).

Gondal, M. A., Li, C., Chang, X., Sikong, L., Yamani, Z. H., Zhou, Q., Yang, F. and Lin, Q., Facile preparation of magnetic C/TiO(2)/Ni composites and their photocatalytic performance for removal of a dye from water under UV light irradiation. J. Environ. Sci. Health. Part A Toxic/Hazard. Subst. Environ. Eng., 47, 570 (2012).

Gurses, A., Dogar, C., Yalcin, M., Acikyildiz, M., Bayrak, R. and Karaca, S., The adsorption kinetics of the cationic dye, methylene blue, onto clay. J. Hazard. Mater., 131, 217 (2006).

Hameed, B. H. and Ahmad, A. A., Batch adsorption of methylene blue from aqueous solution by garlic peel, an agricultural waste biomass. J. Hazard. Mater., 164, 870 (2009).

Ho, Y. S. and McKay, G., A comparison of chermosorption kinetic models applied to pollutant removal on various sorbents. Process Saf. Environ., 76, 332 (1998a).

Ho, Y. S. and McKay, G., The kinetics of sorption of basic dyes from aqueous solution by sphagnum moss peat. Braz. J. Chem. Eng., 76, 822 (1998b).

Karaca, S., Gürses, A., Açikyildiz, M. and Ejder, M., Adsorption of cationic dye from aqueous solutions by activated carbon. Micropor. Mesopor. Mat., 115, 376 (2008).

Khaled, A., El Nemr, A., El-Sikaily, A. and Abdelwahab, O., Removal of Direct N Blue-106 from artificial textile dye effluent using activated carbon from orange peel: adsorption isotherm and kinetic studies. J. Hazard. Mater., 165, 100 (2009).

Kim, H. and Guiochon, G., Adsorption on molecularly imprinted polymers of structural analogues of a template. Single-component adsorption isotherm data. Anal. Chem., 77, 6415 (2005).

Kuleyin, A. and Aydin, F., Removal of reactive textile dyes (Remazol Brillant Blue R and Remazol Yellow) by surfactant-modified natural zeolite. Environ. Prog. Sustain. Energy, 30, 141 (2011).

Kumar, M. N. V. R., Sridhari, T. R., Bhavani, K. D. and Dutta, P. K., Trends in color removal from textile mill effluents. Colorage, 40, 25 (1998).

Lagergren, S. and Svenska, B. K., About the theory of so-called adsorption of soluble substance. Vetenskapsaka. Handl., 24, 1 (1898).

Laidler, K. and Meiser, J. H., Physical Chemistry. Houghton Mifflin New York, 852 (1999).

Langmuir, I., The adsorption of gases on plane surfaces of glass, mica and platinum. J. American Chem. Soc., 40, 1361 (1918).

Li, S., Liu, X., Zou, T. and Xiao, W., Removal of cationic dye from aqueous solution by a macroporous hydrophobically modified poly(acrylic acid-acrylamide) hydrogel with enhanced swelling and adsorption properties. CLEAN – Soil Air Water, 38, 378 (2010).

Lin, J. X., Zhan, S. L., Fang, M. H., Qian, X. Q. and Yang, H., Adsorption of basic dye from aqueous solution onto fly ash. J. Environ. Manage., 87, 193 (2008).

Mafra, M. R., Igarashi-Mafra, L., Zuim, D. R., Vasques, É. C., Ferreira, M. A., Adsorption of remazol brilliant blue on an orange peel adsorbent. Braz. J. Chem. Eng., 30, 657 (2013).

Mahmoodi, N. M., Equilibrium, kinetics, and thermodynamics of dye removal using alginate in binary systems. J. Chem. Eng. Data, 56, 2802 (2011).

Man, L. W., Kumar, P., Teng, T. T. and Wasewar, K. L., Design of experiments for Malachite Green dye removal from wastewater using thermolysis–coagulation–flocculation. Desalin. Water Treat., 40, 260 (2012).

Mesko, V., Markovska, L., Minceva, M. and Burevski, D., Equilibrium isotherms for adsorption of basic dyes from aqueous solutions on different adsorbents. Macedonian J. Chem. Chem. Eng., 20, 143 (2001).

Molinari, R., Pirillo, F., Falco, M., Loddo, V. and

Palmisano, L., Photocatalytic degradation of dyes by using a membrane reactor. Chem. Eng. Process. Process Intensif., 43, 1103 (2004).

Nollet, H., Roels, M., Lutgen, P., Van der Meeren, P. and Verstraete, W., Removal of PCBs from wastewater using fly ash. Chemosphere, 53, 655 (2003).

Pentari, D., Perdikatsis, V., Katsimicha, D. and Kanaki, A., Sorption properties of low calorific value Greek lignites: Removal of lead, cadmium, zinc and copper ions from aqueous solutions. J. Hazard. Mater., 168, 1017 (2009).

Piccin, J. S., Dotto, G. L., Pinto, L. A. A., Adsorption isotherms and thermochemical data of FD&C Red n° 40 binding by Chitosan. Braz. J. Chem. Eng., 28, 295 (2011).

Rashidian, M., Dorranian, D., Ahmadi Darani, S., Saghafi, S. and Ghoranneviss, M., Nonlinear responses and optical limiting behavior of Basic Violet 16 dye under CW laser illumination. Optik, 120, 1000 (2009).

Schimmel, D., Fagnani, K. C., Oliveira dos Santos. J. B., Barros, M. A. S. D., Antonio da Silva, E., Adsorption of turquoise blue QG reactive bye commercial activated carbon in batch reactor: Kinetic and equilibrium studies. Braz. J. Chem. Eng., 27, 289 (2010).

Somasekhara Reddy, M. C., Sivaramakrishna, L. and Varada Reddy, A., The use of an agricultural waste material, Jujuba seeds for the removal of anionic dye (Congo Red) from aqueous medium. J. Hazard. Mater., 203-204, 118 (2012).

Tehrani-Bagha, A. R., Nikkar, H., Mahmoodi, N. M., Markazi, M. and Menger, F. M., The sorption of cationic dyes onto kaolin: Kinetic, isotherm and thermodynamic studies. Desalination, 266, 274 (2011).

Temkin, M. I., Adsorption equilibrium and the kinetics of processes on non-homogeneous surfaces and in the interaction between adsorbed molecules. Zh. Fiz. Khim., 15, 296 (1941).

Ugurlu, M. and Karaoglu, M. H., Adsorption of ammonium from an aqueous solution by fly ash and sepiolite: Isotherm, kinetic and thermodynamic analysis. Micropor. Mesopor. Mat., 139, 173 (2011).

van Leeuwen, J., Sridhar, A., Esplugas, M., Onuki, S., Cai, L. and Koziel, J. A., Ozonation within an activated sludge system for azo dye removal by partial oxidation and biodegradation. Ozone Sci. Eng., 31, 279 (2009).

Varlikli, C., Bekiari, V., Kus, M., Boduroglu, N., Oner, I., Lianos, P., Lyberatos, G. and Icli, S., Adsorption of dyes on Sahara desert sand. J. Hazard. Mater., 170, 27 (2009).

Vimonses, V., Lei, S., Jin, B., Chow, C. W. K. and Saint, C., Kinetic study and equilibrium isotherm analysis of Congo Red adsorption by clay materials. Chem. Eng. J., 148, 354 (2009).

Vučurović, V. M., Razmovski, R. N. and Tekić, M. N., Methylene blue (cationic dye) adsorption onto sugar beet pulp: Equilibrium isotherm and kinetic studies. J. Taiwan Inst. Chem. Eng., 43, 108 (2012).

Weber, W. J. and Morris, J. C., Kinetics of adsorption on carbon from solution. J. Sanit. Eng. Div. Proceed. American Soc. Civ. Eng., 89, 31 (1963).

Weng, C. H., Lin, Y. T. and Tzeng, T. W., Removal of methylene blue from aqueous solution by adsorption onto pineapple leaf powder. J. Hazard. Mater., 170, 417 (2009).

Yousef, R. I., El-Eswed, B. and Al-Muhtaseb, A. a. H., Adsorption characteristics of natural zeolites as solid adsorbents for phenol removal from aqueous solutions: Kinetics, mechanism, and thermodynamics studies. Chem. Eng. J., 171, 1143 (2011).